Carbohydrate Polymers 102 (2014) 846–851

Contents lists available at ScienceDirect

Carbohydrate Polymers

journal homepage: www.elsevier.com/locate/carbpol

Mineralization of hydroxyapatite upon a unique xanthan gum hydrogel by an alternate soaking process

Hironori Izawa[a,*], Shoji Nishino[a], Hiroyuki Maeda[a], Kohei Morita[a], Shinsuke Ifuku[a], Minoru Morimoto[a], Hiroyuki Saimoto[a], Jun-ichi Kadokawa[b,c]

[a] Graduate School of Engineering, Tottori University, 4-101 Koyama-Minami, Tottori 680-8550, Japan
[b] Graduate School of Science and Engineering, Kagoshima University, 1-21-40 Korimoto, Kagoshima 890-0065, Japan
[c] Research Center for Environmentally Friendly Materials Engineering, Muroran Institute of Technology, 27-1 Mizumoto-cho, Muroran, Hokkaido 050-8585, Japan

ARTICLE INFO

Article history:
Received 12 July 2013
Received in revised form 22 October 2013
Accepted 28 October 2013
Available online 5 November 2013

Keywords:
Xanthan gum
Hydroxyapatite
Alternate soaking process
Inorganic–organic composite hydrogel
Mineralization

ABSTRACT

We previously reported a xanthan gum (Xan) hydrogel showing excellent mechanical properties. Mineralization of hydroxyapatite (Hap) upon the Xan hydrogel would provide a unique biomaterial applicable for bone tissue engineering. Here, we show the mineralization of Hap upon the Xan hydrogel by means of an alternate soaking process. Hap was gradually grown upon the Xan-matrix surface with increasing number of soaking cycles due to the ionic interactions between calcium cations and carboxyl groups. Interestingly, the mineralization induced a microstructure change in the gel-matrix from a layered structure to a porous structure. The mechanical properties of the resulting Hap–Xan composite hydrogels were further investigated by a tensile test, where the Hap–Xan composite hydrogel with an appropriate amount of Hap (Xan/Hap = 2.7) was capable of approximately 370% elongation.

1. Introduction

Biomineralization is a widespread phenomenon in nature leading to the formation of a variety of solid inorganic structures by living organisms (Arias & Fernandez, 2008), in which finely scaled and highly controlled inorganic precipitates are generated in organic matrixes through self-assembled bottom-up processes under mild conditions (Calvert & Rieke, 1996). These biologically produced biominerals are inorganic–organic hybrid composites showing interesting properties, including controlled hierarchical structures and remodeling or repair mechanisms that remain to be developed into a practical engineering process (Dujardin & Mann, 2002; Heuer et al., 1992; Mann, 2000). Thus, biomimetic mineralization has been emerging as an active area of recent research for the design of new materials and devices in various fields (Colfen, 2007).

Hydroxyapatite (Hap) ($Ca_{10}(PO_4)_6(OH)_2$) is the inorganic component of hard tissues of vertebrate. Hap exhibits excellent biocompatibility with various kinds of cells and tissues (Okada & Furuzono, 2012). The Hap-polymer composite, mimicking the composition and structure of mineralized tissues, provides excellent mechanical properties in addition to favorable biological properties, making it an ideal candidate for tissue engineering as well as orthopedic and dental applications (Sun, Zhou, & Lee, 2011). Anionic polysaccharides such as alginate, hyaluronic acid, and chondroitin sulfate are potential optimal templates for the mineralization of Hap because their anionic surface can bind Ca^{2+} ions and can control crystal nucleation and growth by lowering the interfacial energy between the crystal and the surface (Arias & Fernandez, 2008). Therefore, various Hap-composited materials have been prepared by using anionic polysaccharides for biomedical applications, including bone tissue engineering (Chen, Ushida, & Tateishi, 2002; Du, Song, Cui, Yang, & Li, 2011; Green et al., 2005; Shi, Zhang, Qi, & Cao, 2012; Shi, Zhang, Yang, & Tang, 2009; Zhong & Chu, 2012).

Xanthan gum (Xan), which is a water-soluble anionic polysaccharide produced by *Xanthomonas campestris*, is a useful food hydrocolloid (Jansson, Kenne, & Lindberg, 1975). It has a cellulose main-chain ((1/4)-β-glucan) with trisaccharide anionic sidechains attached to alternate glucose units in the main-chain (Melton, Mindt, Rees, & Sanderson, 1976). Xan has been widely used in a broad range of industries as a rheological control agent in aqueous systems and as a stabilizer for emulsions and suspensions (Rosalam & England, 2006). In general, an aqueous dispersion of Xan exhibits only weak gel-like behavior in the presence of a sufficient amount of inorganic salt because it is a micro-gel with a double-helix conformation (Alistair, Glyn, & Peter, 2006). We have discovered, however, that Xan can be converted to a Xan hydrogel with

* Corresponding author at: Department of Science and Biotechnology, Graduate School of Engineering, Tottori University, 4-101 Koyama-Minami, Tottori 680-8550, Japan. Tel.: +81 857 31 5813; fax: +81 857 31 5813.
E-mail address: h-izawa@chem.tottori-u.ac.jp (H. Izawa).

0144-8617/$ – see front matter © 2013 Elsevier Ltd. All rights reserved.
http://dx.doi.org/10.1016/j.carbpol.2013.10.080

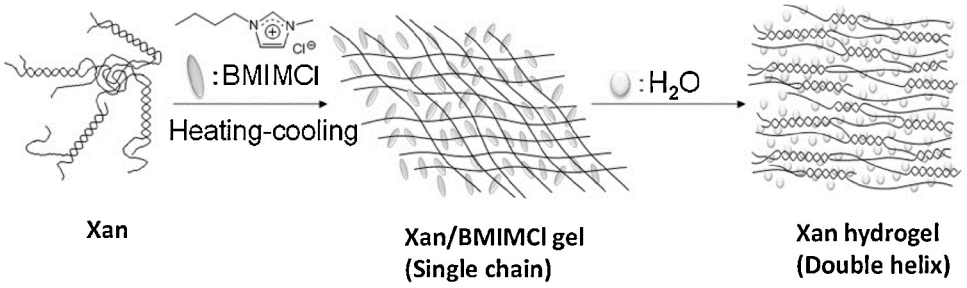

Fig. 1. Preparation of the Xan hydrogel with BMIMCl.

excellent mechanical properties by means of a gelation process with 1-butyl-3-methylimidazolium chloride (BMIMCl) (Fig. 1) (Izawa & Kadokawa, 2010; Izawa, Kaneko, & Kadokawa, 2009). When Xan is heated at 100 °C in BMIMCl, the double-helix conformation of Xan is disentangled, resulting in dissolution. Subsequent cooling of the Xan/BMIMCl solution to room temperature then induces gelation. The Xan/BMIMCl gel was soaked in a large volume of pure water to create the Xan hydrogel, in which the double-helix conformation of Xan was restored in response to the high ionic strength (Camesano & Wilkinson, 2001). Although the chemical structure of Xan did not change during the gelling process, the Xan hydrogel was surprisingly capable of approximately 500% strain in the tensile test (Izawa & Kadokawa, 2010). Such a polysaccharide hydrogel having both a tough and elastic nature is quite rare. In addition, the Xan hydrogel can potentially serve as an organic template for biomimetic mineralization because Xan has carboxyl groups in its residue. The mineralization of Hap upon a Xan-matrix surface would provide a high performance Hap-composited hydrogel applicable to bone tissue engineering. Here we show the mineralization of Hap upon the Xan hydrogel. The Xan hydrogel prepared by using BMIMCl was subjected to an alternate soaking process (Taguchi, Kishida, & Akashi, 1998). The resulting Hap–Xan composite hydrogel was evaluated by infrared spectroscopy (IR), X-ray diffraction spectroscopy (XRD), scanning electron microscopy (SEM), and energy-dispersive X-ray spectrometry (EDX) analyses. The mechanical properties of the Hap–Xan composite hydrogel were further investigated by tensile test.

2. Experiments

2.1. Materials

BMIMCl was purchased from Sigma–Aldrich Japan (Tokyo, Japan). Xan (viscosity; 1785 cps, 1 wt.% solution in 1 wt.% KCl aq., 20 °C) was purchased from Tokyo Chemical Industry Co., Ltd. (Tokyo, Japan). Commercial products of Xan have a moisture content of ca. 11% and an ash content of 6–9% (Alistair et al., 2006). The molecular weights of the Xan samples are generally 2–50 × 10^6 Da (Alistair et al., 2006). Other reagents were used as commercial grade without further purification.

2.2. Preparation of the Xan hydrogel

Xan (0.10 g, i.e., 9.1 wt.%) was added to BMIMCl (1.00 g) and stirred for 3 min at 100 °C to create a homogeneous solution. After the solution was continuously heated at 100 °C for 12 h without stirring to completely dissolve Xan, it was kept at room temperature for 30 min to give a xanthan/BMIMCl gel. The Xan/BMIMCl gel was compressed at 100 °C for 10 min by hot-pressing with a 0.5 mm thick spacer to create a film gel. The Xan/BMIMCl gel film was soaked in pure water (100 mL) at 5 °C for 12 h. The Xan hydrogel was picked up from the water and was subsequently soaked in 0.5 M $CaCl_2$ aqueous solution (10 mL) at 5 °C for 12 h, followed by soaking in pure water (100 mL) for 12 h at 5 °C.

2.3. Preparation of the Hap–Xan composite hydrogel

Conditions for the alternate soaking process were utilized as reported previously (Ngiam, Liao, Patil, Cheng, Chan, & Ramakrishna, 2009). The Xan hydrogel was first soaked in 0.3 M Na_2HPO_4 aqueous solution (10 mL) at 37 °C for 1 h, followed by soaking in pure water (100 mL) for 1 h at room temperature. Next, the Xan hydrogel was soaked in 0.5 M $CaCl_2$ aqueous solution (10 mL) at 37 °C for 1 h, followed by soaking in pure water (100 mL) for 1 h at room temperature. This alternate soaking cycle was repeated for 5 or 10 cycles.

2.4. Measurements

Infrared spectra of the samples were recorded with an FT-IR spectrophotometer (Spectrum 65, Perkin-Elmer Japan Co., Ltd., Japan) equipped with an ATR attachment. X-ray diffraction profiles were obtained with Ni-filtered CuKα from an X-ray generator (Ultima IV, Rigaku, Japan) operating at 40 kV and 30 mA. The diffraction profile was detected using an X-ray goniometer scanning from 10° to 60°. For field emission scanning electron microscopic (FE-SEM) observation, the sample was coated with an approximately 2 nm layer of Pt by an ion sputter coater and observed by FE-SEM (JSM-6700F; JEOL, Ltd., Japan), equipped with energy dispersive X-ray microanalyzer (JED-2200, JEOL Ltd., Japan), operating at 2.0 kV. EDX spectrum was measured without Pt-coating. Tensile strengths and Young's moduli were measured by a universal testing instrument (AG-10KNX, Shimadzu, Japan) for samples 50 mm long and 10 mm wide at a cross head speed of 1 mm min^{-1} with a gage length of 30 mm.

3. Results and discussion

3.1. Preparation of the Hap–Xan composite hydrogel

The Xan/BMIMCl gel (9.1 wt.%) was prepared by the previously reported method (Fig. 2a) (Izawa & Kadokawa, 2010). When the Xan hydrogel was subjected to the alternate soaking process, the Xan hydrogel was allowed to reach equilibrium in the solutions. Film shape enabled equilibration with a shorter soaking time because of the larger contact area to water. The Xan/BMIMCl gel was therefore processed into a gel film (ca 0.5 mm thick) by hot-pressing. The Xan/BMIMCl film gel was subsequently converted to a Xan hydrogel by soaking in a large volume of pure water. The hydrogel was ion-exchanged to Ca^{2+}. Residual salt in the Xan hydrogel was removed by soaking in a large volume of pure water.

Next, mineralization of Hap upon the Xan hydrogel by the alternate soaking process was investigated (Fig. 2b). The Xan hydrogel gradually turned white with soaking cycles of increasing length

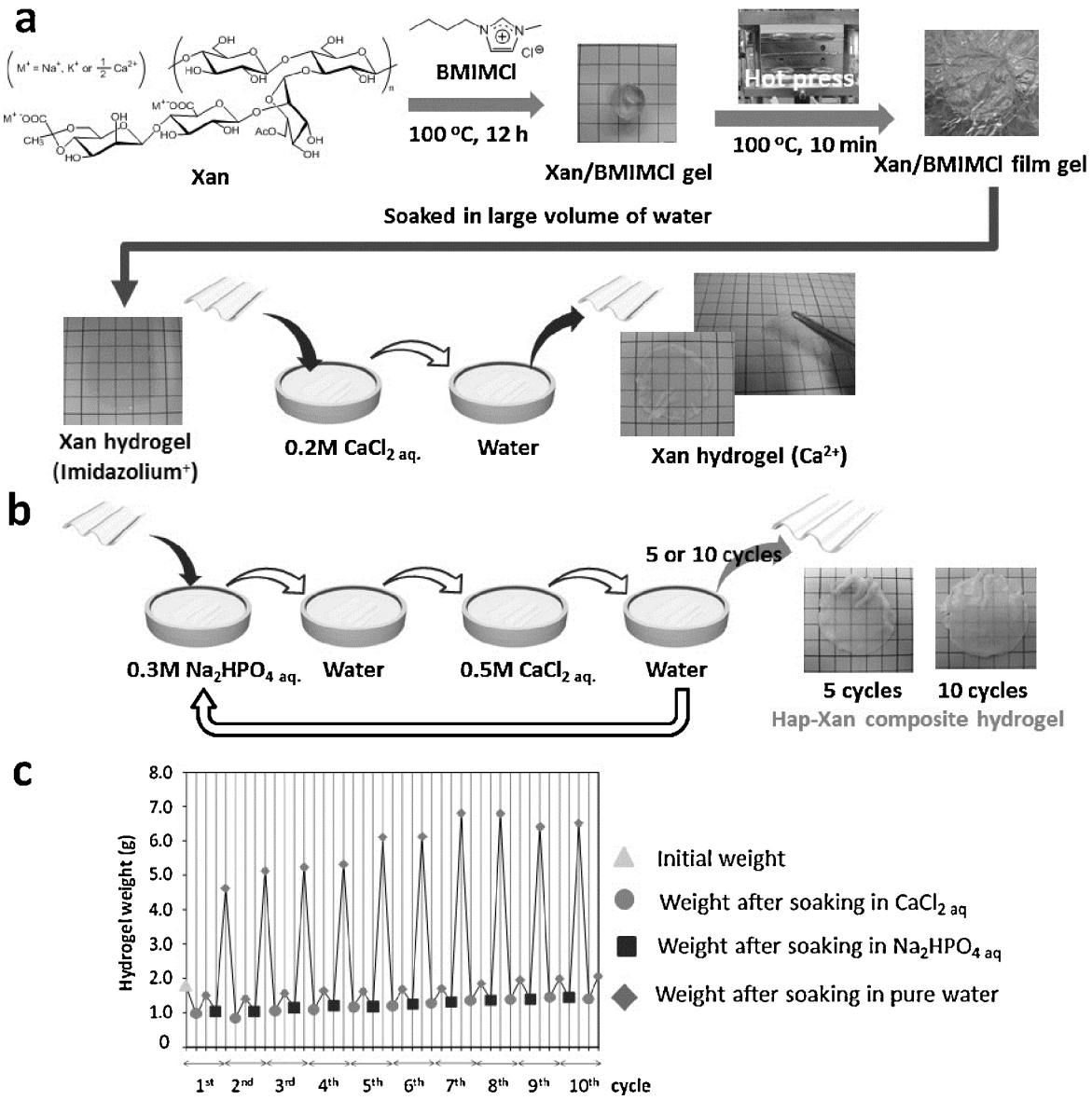

Fig. 2. Preparation of the Hap–Xan composite hydrogel by the alternate soaking process. Schematic image of preparation of the Xan hydrogel (Ca^{2+}) (a) and the alternate soaking process (b). Hydrogel weight during the alternate soaking process (c).

due to the mineralization of Hap. Interestingly, the weights of the hydrogels were reversibly changed during the alternate soaking process (Fig. 2c). When the hydrogel was soaked in pure water, it immediately swelled, whereas the swollen volume after soaking in $CaCl_2$ aqueous solution was much smaller than that after soaking in Na_2HPO_4 aqueous solution due to the ionic crosslinking of Ca^{2+}. In contrast, the swollen hydrogel immediately shrunk in Na_2HPO_4 and $CaCl_2$ aqueous solution. This behavior is similar to previously reported swelling–shrinking behavior of the Xan hydrogel (Izawa & Kadokawa, 2010). As described in the introduction, the conformation of Xan is reversibly changed from a double-helix to a single chain in response to a high or low ionic strength (Camesano & Wilkinson, 2001), which caused reversible swelling–shrinking behavior of the Xan hydrogel (Izawa & Kadokawa, 2010). In addition, the weight of the initial Xan hydrogel (Ca^{2+} form) after soaking in pure water in the first cycle increased to ca 1.5 times after 10 cycles. It is thought that this increase was caused by a reduction in the quantity of the double-helix part in the Xan-matrix as described hereinafter.

3.2. Analysis of the Hap–Xan composite hydrogel

IR and XRD analyses of lyophilized-composite hydrogels were investigated to confirm the production of Hap. Fig. 3a shows the IR spectra of the lyophilized-Xan hydrogel (blank) and the Hap–Xan composite hydrogel obtained by 5- or 10-cycles (a so-called 5- or 10-cycle gel, respectively). The absorption peaks due to PO_4^{3-} for Hap are shown at 570 cm^{-1}, 603 cm^{-1}, 962 cm^{-1}, and 1045 cm^{-1} (Tas, 2000). Although the absorption peaks at 962 cm^{-1} and 1045 cm^{-1} were overlapped with those of Xan, the absorption peaks at 570 cm^{-1} and 603 cm^{-1} (pointed by arrows) were clearly observed in the 5- and 10-cycle gels, which is suggestive of the production of Hap. Fig. 3b shows XRD patterns of blank and 5- and 10-cycle gels. In the spectrum of the blank, the broad diffraction peak corresponding to the double-helix conformation of Xan was only observed at around 20° (Alistair et al., 2006; Millane & Narasaiah, 1990; Moorhouse, Walkinshaw, & Arnott, 1977). In contrast, in those of the 5- and 10-cycle gels, distinct diffraction peaks were observed at 25.9°, 28.3°, 33.5°, 38.9°, 46.3°, 49.3°, and 53.2°

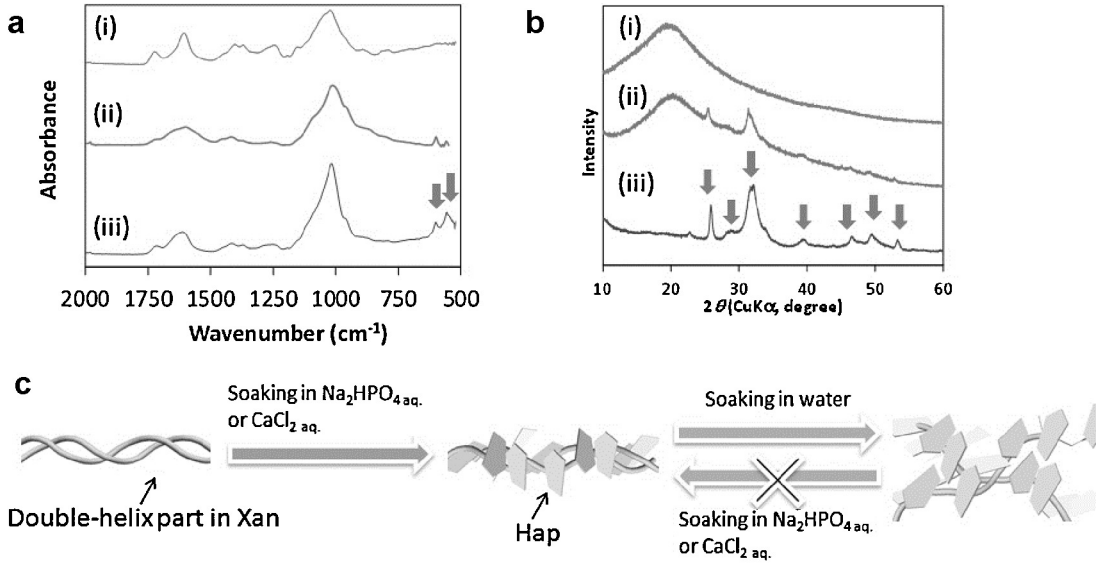

Fig. 3. IR spectra of the blank (i) and 5- (ii) and 10-cycle gels (iii) (a) and XRD patterns of the blank (i), 5- (ii) and 10-cycle gels (iii) (b). Plausible mechanism for reduction of the double-helix part (c).

(pointed by arrows) in agreement with the reported diffraction peaks for Hap (Tas, 2000), indicating production of Hap upon the Xan hydrogel. On the other hand, the broad diffraction peak due to the double-helix conformation of Xan gradually disappeared with increases in the number of soaking cycles, suggesting that the mineralization of Hap upon the Xan hydrogel involves a reduction of the double-helix part of the Xan-matrix. This result is consistent with the aforementioned swelling behavior being dependent on the soaking cycles because the decreasing quantity of the double-helix part presenting as a junction zone allows water absorption. The reason for the reduction in the double-helix part is thought to be that Hap-deposited Xan single chains cannot restore the double-helix conformation because of the hindrance of Hap (Fig. 3c).

Fig. 4 shows SEM images of the cross-sections of the lyophilized hydrogels. A multi-layered structure was observed in the blank (Fig. 4a), whereas the microstructure was dramatically changed after mineralization. In the 5-cycle gel, a porous structure composed of nano-flakes was observed (Fig. 4b). The nano-flakes were grown by further soaking up to 10 cycles (Fig. 4c). To confirm the composition of the nano-flakes, EDX analysis was investigated (Fig. 4f). In the EDX spectrum, the presence of Ca, P, and O was observed, suggesting that the nano-flakes were definitely Hap. In addition, the Ca/P atomic ratio was estimated to be 1.65, which was slightly lower than the theoretical Ca/P atomic ratio of Hap ($Ca_{10}(PO_4)_6(OH)_2$; 1.67). The chemical formula estimated from the Ca/P ratio was ($Ca_{9.9}(HPO_4)_{0.1}(PO_4)_{5.9}(OH)_2$), which was classified as calcium-deficient Hap (Okada & Furuzono, 2012). Note that SEM images of the Hap–Xan composite hydrogel surface are almost the same as the aforementioned cross-sectional images, indicating that the Hap–Xan composite hydrogels were completely equilibrated during the alternate soaking process.

Although Hap was observed in the SEM analysis of the 5- and 10-cycle gels, the Xan-matrix was not recognized. We supposed that the Xan-matrix was completely hidden behind the Hap-flakes. SEM analysis of a 1-cycle gel with a Xan/Hap ratio of 15.4 was therefore carried out (Fig. 4d). Interestingly, a structure change from a

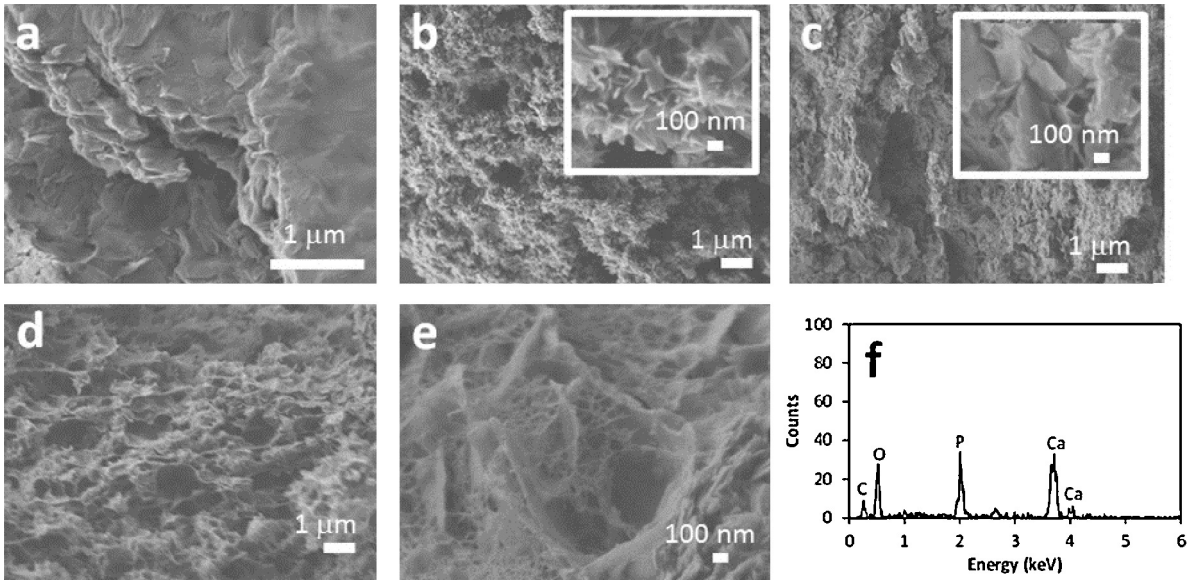

Fig. 4. SEM images of blank (a), 5-cycle gel (b), 10-cycle gel (c), 1-cycle gel (d), and the swelled-10-cycle gel (e). EDX spectrum of the 5-cycle gel (f).

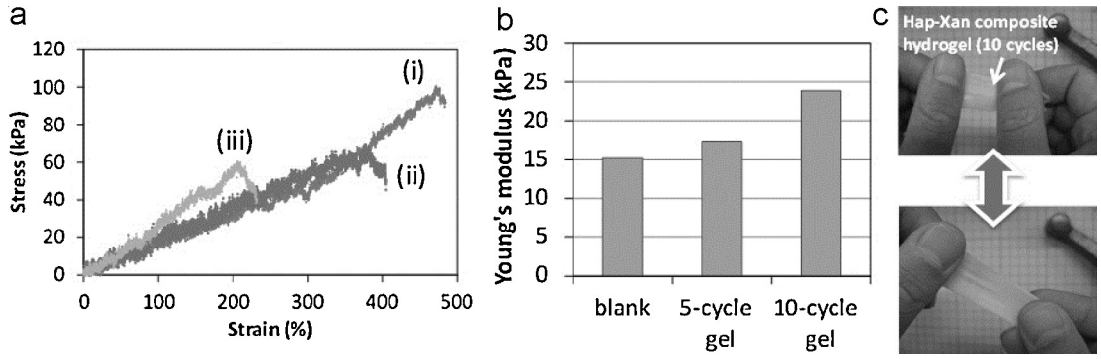

Fig. 5. Stress-strain curves (a) and Young's moduli (b) of blank (i), 5- (ii) and 10-cycle gels (iii). An image of the elongated-10 cycle gel (c).

layered to a porous structure was observed at this stage, indicating that the microstructure change was induced even by the slight nucleation and was caused by the morphology change of the Xan-matrix due to mineralization. SEM analysis of the swelling-gel (Na^+ form) obtained after soaking in pure water during the 10th cycle was further investigated (Fig. 4e), with nano-fibrils (ca 10 nm) of Xan being observed on the space between the Hap-flakes. This result suggests that the Xan-matrix was completely adhering to the Hap-surface through ionic interactions in the case of the Ca^{2+} form, and it therefore was not observed in the SEM analysis.

The Hap contents of the 5- and 10-cycle gels were estimated by the difference in the weight of the dried-blank and dried-5- and 10-cycle gels, respectively. The Hap contents of the 5- and 10-cycle gels were 1.9% and 4.8%, respectively, which was clearly dependent on the number of soaking cycles. This result is consistent with the results in the SEM analysis where the Hap amount of the 10-cycle gel was obviously greater than that of the 5-cycle gel. The water content was estimated by the difference in the weight of the hydrogel and that of the dried-material. The water contents of the 5- and 10-cycle gels were 93.0% and 91.2%, respectively, which were higher than that of the blank (89.9%). The result is probably due to the decreased quantity of the double-helix part in the Xan-matrix, as mentioned above.

3.3. Mechanical properties of the Hap–Xan composite hydrogel

Fig. 5a shows the stress–strain curves of the blank and 5- and 10-cycle gels under tensile mode. The fracture stress and strain of the blank were 99.8 kPa and 471.3%, respectively. These values were similar to those reported previously (Izawa et al., 2009). Unfortunately, however, those of the 5- and 10-cycle gels were reduced to 68.9 kPa and 376.4% and 59.8 kPa and 204.8%, respectively. This reduction in mechanical strength was probably caused by the decreased quantity of the double-helix part, as the presence of a junction point generally enhances the gel strength (Kuo & Ma, 2008). On the other hand, Young's modulus was increased with increasing amounts of Hap, with values for the 5- and 10-cycle gels being 1.1 or 1.6 times that of the blank, respectively (Fig. 5b). Thus, it is supposed that the fracture stress of the Hap–Xan composite hydrogel depends on the quantity of the double-helix part of the Xan-matrix. In contrast, increasing amounts of Hap slightly enhance the Young's modulus. It should be noted that although mechanical strength was reduced by the mineralization as compared to the blank, the strength remained high, as shown in Fig. 5c. Typical polysaccharide gels do not show such elasticity.

4. Conclusion

In this study, Hap was successfully mineralized upon the Xan hydrogel by the alternate soaking process, where the Xan-matrix worked as a scaffold due to the presence of carboxyl groups. The content of Hap in the Hap–Xan composite hydrogel was clearly dependent on the soaking cycles. Interestingly, the mineralization of Hap induced a microstructure change of the Xan hydrogel from a layered structure to a porous structure. In addition, the double-helix part of the Xan hydrogel decreased with increases in the number of soaking cycles because the produced-Hap avoided restoration of the double-helix conformation. Furthermore, the mechanical properties of the Hap–Xan composite hydrogel were investigated by the tensile test. Although the mechanical strength of the Hap–Xan composite hydrogel was reduced with increasing the number of soaking cycles, the mechanical strength remained high even after 5 or 10 cycles, which allowed for approximately 380 and 200% elongation, respectively. There have previously been no reports of such elastic Hap-composited hydrogels. This Hap–Xan composite hydrogel showing unique mechanical properties would be a powerful tool for a scaffold material for bone tissue engineering (Chen et al., 2002). In addition, the Hap–Xan composite material is applicable for use as a force-responsive material in mechanobiochemistry (Brantley, Bailey, Wiggins, Keatinge-Clay, & Bielawski, 2013) to provide new scientific knowledge.

Acknowledgement

This work was in part supported by the Tottori Prefecture Environment and Academic Promotion Project.

References

Alistair, M. S., Glyn, O. P., & Peter, A. W. (Eds.). (2006). *Food polysaccharides and their applications*. London: CRC press.
Arias, J. L., & Fernandez, M. S. (2008). Polysaccharides and proteoglycans in calcium carbonate-based biomineralization. *Chemical Reviews*, *108*(11), 4475–4482.
Brantley, J. N., Bailey, C. B., Wiggins, K. M., Keatinge-Clay, A. T., & Bielawski, C. W. (2013). Mechanobiochemistry: Harnessing biomacromolecules for force-responsive materials. *Polymer Chemistry*, *4*, 3916–3928.
Calvert, P., & Rieke, P. (1996). Biomimetic mineralization in and on polymers. *Chemistry of Materials*, *8*(8), 1715–1727.
Camesano, T. A., & Wilkinson, K. J. (2001). Single molecule study of xanthan conformation using atomic force microscopy. *Biomacromolecules*, *2*(4), 1184–1191.
Chen, G. P., Ushida, T., & Tateishi, T. (2002). Scaffold design for tissue engineering. *Macromolecular Bioscience*, *2*(2), 67–77.
Colfen, H. (2007). Bio-inspired mineralization using hydrophilic polymers. *Topics in Current Chemistry*, *271*, 1–77.
Du, M. C., Song, W. X., Cui, Y., Yang, Y., & Li, J. B. (2011). Fabrication and biological application of nano-hydroxyapatite (nHA)/alginate (ALG) hydrogel as scaffolds. *Journal of Materials Chemistry*, *21*(7), 2228–2236.
Dujardin, E., & Mann, S. (2002). Bio-inspired materials chemistry. *Advanced Materials*, *14*(11), 775–788.
Green, D. W., Leveque, I., Walsh, D., Howard, D., Yang, X. B., Partridge, K., Mann, S., & Oreffo, R. O. C. (2005). Biomineralized polysaccharide capsules for encapsulation, organization, and delivery of human cell types and growth factors. *Advanced Functional Materials*, *15*(6), 917–923.
Heuer, A. H., Fink, D. J., Laraia, V. J., Arias, J. L., Calvert, P. D., Kendall, K., Messing, G. L., Blackwell, J., Rieke, P. C., Thompson, D. H., Wheeler, A. P., Veis, A., & Caplan, A. I. (1992). Innovative materials processing strategies – A biomimetic approach. *Science*, *255*(5048), 1098–1105.

Izawa, H., & Kadokawa, J. (2010). Preparation and characterizations of functional ionic liquid–gel and hydrogel materials of xanthan gum. *Journal of Materials Chemistry*, *20*(25), 5235–5241.

Izawa, H., Kaneko, Y., & Kadokawa, J. (2009). Unique gel of xanthan gum with ionic liquid and its conversion into high performance hydrogel. *Journal of Materials Chemistry*, *19*(38), 6969–6972.

Jansson, P. E., Kenne, L., & Lindberg, B. (1975). Structure of extracellular polysaccharide from *Xanthomonas campestris*. *Carbohydrate Research*, *45*(Dec), 275L 282.

Kuo, C. K., & Ma, P. X. (2008). Maintaining dimensions and mechanical properties of ionically crosslinked alginate hydrogel scaffolds in vitro. *Journal of Biomedical Materials Research Part A*, *84A*(4), 899–907.

Mann, S. (2000). The chemistry of form. *Angewandte Chemie International Edition*, *39*(19), 3393–3406.

Melton, L. D., Mindt, L., Rees, D. A., & Sanderson, G. R. (1976). Covalent structure of extracellular polysaccharide from xanthomonas-campestris – Evidence from partial hydrolysis studies. *Carbohydrate Research*, *46*(2), 245–257.

Millane, R. P., & Narasaiah, T. V. (1990). X-ray fiber diffraction studies of a variant of xanthan gum in which the sidechain terminal mannose unit is absent. *Carbohydrate Polymers*, *12*(3), 315–321.

Moorhouse, R., Walkinshaw, M. D., & Arnott, S. (1977). *Xanthan gum—Molecular conformation and interactions*. Washington, DC: American Chemical Society.

Ngiam, M., Liao, S. S., Patil, A. J., Cheng, Z. Y., Chan, C. K., & Ramakrishna, S. (2009). The fabrication of nano-hydroxyapatite on PLGA and PLGA/collagen nanofibrous composite scaffolds and their effects in osteoblastic behavior for bone tissue engineering. *Bone*, *45*(1), 4–16.

Okada, M., & Furuzono, T. (2012). Hydroxylapatite nanoparticles: Fabrication methods and medical applications. *Science and Technology of Advanced Materials*, *13*(6).

Rosalam, S., & England, R. (2006). Review of xanthan gum production from unmodified starches by *Xanthomonas comprestris* sp. *Enzyme and Microbial Technology*, *39*(2), 197–207.

Shi, Y., Zhang, Y. H., Yang, W. L., & Tang, Y. (2009). Multiradiate calcium phosphate patterns derived from a gradating polysaccharide-acidic protein system. *Chemical Communications*, (4), 442–444.

Shi, J., Zhang, Z. Z., Qi, W. Y., & Cao, S. K. (2012). Hydrophobically modified biomineralized polysaccharide alginate membrane for sustained smart drug delivery. *International Journal of Biological Macromolecules*, *50*(3), 747–753.

Sun, F., Zhou, H., & Lee, J. (2011). Various preparation methods of highly porous hydroxyapatite/polymer nanoscale biocomposites for bone regeneration. *Acta Biomaterialia*, *7*(11), 3813–3828.

Taguchi, T., Kishida, A., & Akashi, M. (1998). Hydroxyapatite formation on/in poly(vinyl alcohol) hydrogel matrices using a novel alternate soaking process. *Chemistry Letters*, (8), 711–712.

Tas, A. C. (2000). Synthesis of biomimetic Ca-hydroxyapatite powders at 37 degrees C in synthetic body fluids. *Biomaterials*, *21*(14), 1429–1438.

Zhong, C., & Chu, C. C. (2012). Biomimetic mineralization of acid polysaccharide-based hydrogels: Towards porous 3-dimensional bone-like biocomposites. *Journal of Materials Chemistry*, *22*(13), 6080–6087.